J Fluoresc (2009) 19:875–880
DOI 10.1007/s10895-009-0486-7

ORIGINAL PAPER

Fluorescence Photobleaching Recovery Method with Pulse-Position Modulation of Bleaching/Probing Irradiation

Yu I. Glazachev

Received: 7 May 2008 / Accepted: 28 March 2009 / Published online: 8 April 2009

Abstract The fluorescence photobleaching recovery method with pulse-position modulation (PPM) of bleaching/probing irradiation is presented. This approach is modification of previously announced photobleaching recovery under decaying photobleaching (FRDP) approach, which employs the amplitude control of irradiation intensity. Underlying idea was to solve the problem of setup nonlinearity by methodical modification that was successfully done. The irradiation intensity is series of equal bleach-probe pulses with increasing distance. The more sophisticated series was proposed as a convolution of subseries, which one characterizing its own time scale. It allows to detect the fluorescence kinetics in the wide range of time and of different nature simultaneously. The method was applied on model systems as FITC-HSA in the water/glycerol mixture and FITC-DMPE in the POPC multibilayers. The method allowed to detect and investigate diffusion processes, presence immobile fraction, effect of limited area of liposomes and reversible fluorescence kinetics.

Keywords Photobleaching · FITC · Albumin · POPC · Diffusion

Introduction

Previously we announced a modification of fluorescence photobleaching method for investigation of lateral diffusion in the membrane-like structure termed as fluorescence recovery under decaying photobleaching (FRDP) [1]. In this method, the applied irradiation is bleaching/probing and decays with time. It leads to a numerous advantages over classical FRAP, such as an increase of signal-to-noise ratio (25–30 fold), presence of minimum in the observed kinetics etc.

In this method, the intensity of irradiation changes in a wide range (at least, in ten times) that leads to unwanted instrumental features originated mainly from nonlinearity of photomultiplier tube and its background signal. It imposes the limitation on this approach for prolonged kinetics measurement, which diminishes one of the important advantages of the method.

In this work we propose to substitute the analog modulation of irradiation intensity for pulse-position modulation (PPM), which is used to provide high linearity in the control system.

Materials and methods

Instrumental setup

The instrumental setup consists of the fluorescence microscope, photomultiplier tube (PMT) and irradiation source controlled with universal microcontroller as described earlier [1]. In the present modification, instead of argon laser we used the ultra bright light emitting diode (LED) as irradiation source. This LED has the maximum intensity at 455 nm (royal blue in manufacture's terms, LXK2-PR14, LUXEON) with half width of 20 nm with power of irradiation up to about 0.75 Wt. Right after diode the pinhole is located. In the experiment, we used pinhole sizes of 0.9 mm and 0.45 mm. The LED/pinhole unit was located in the focus of microscope that provides a sharp spot on

Y. I. Glazachev (✉)
Institute of Chemical Kinetics and Combustion,
Institutskaya str.3,
Novosibirsk 630090, Russian Federation
e-mail: glaza@kinetics.nsc.ru

the sample. The objective 90× with oil immersion has been used.

Setup allows working both in amplitude and pulse modulation modes. All experimental data were obtained in pulse-position modulation mode. Note that LED is recommended by manufacture to be applied namely in pulse mode. The intensity can be controlled with either direct current of LED or reverse current of photodiode, faced to irradiation.

Sample preparation

The fluorescently labeled human serum albumin (FITC-HSA, modification extent 1.5:1) was used in concentration of one micromole in the glycerol/water mixture (80% w/w, PBS buffer 0.05M, pH8). The sample volume of 5 µl was placed on sample glass covered with cover glass of 24× 24 mm and sealed with paraffin. It yields the thickness of layer ~10 µm. The experiments have been started in 1 h after preparation.

The liposomes were prepared from palmitoyloleoyl phosphocholine (POPC) with addition of FITC labeled dimiristeoyl-phosphatidylethanolamine (FITC-DMPE) as lipid probe. The molar ratio POPC:FITC-DMPE is 70 000:1. The 20 µl of the sample solution in chloroform (0.05M) was placed on sample glass and dried under vacuum for 1–2 h. PBS buffer (10 µl, 0.05M, pH7.5) was added the lipid film, covered by cover glass and sealed. Sample was placed in thermostating unit warmed up to 30 °–35 °C and left for a night under slow cooling to room temperature. Experiments were performed during next day.

Theory

The underlying principle of FRDP method is based on applying of photobleaching/probing irradiation that decays with time course. The analytical solution of the observed kinetics of normalized fluorescence, *f(t),* in the approximation of low bleaching and Gaussian lineshape of beam has been previously obtained [1]:

$$\frac{F(t)}{T(t)} = f(t) = f(0) \cdot \left(1 - B \cdot \int_0^t \frac{T(x)}{1 + \frac{t-x}{t_D}} dx\right) \quad (1)$$

where *F(t)* is kinetics of fluorescence; *T(t)* is intensity of bleaching/probing irradiation; *B* is integral rate of photobleaching (s^{-1}); t_D is characteristic diffusion time.

As the optimal function for *T(t)* was proposed the hyperbolic decay:

$$T(t) = \frac{1}{1 + t/t_B} \quad (2)$$

where t_B is characteristic time of irradiation decay. This value is considered as time scale parameter for irradiation function. The normalized fluorescence now evaluates to [1]:

$$\frac{f(t)}{f(0)} = 1 - B_D \cdot \frac{t_B \cdot t_D}{t_B + t_D + t} \cdot \left\{ \ln\left|1 + \frac{t}{t_B}\right| + \ln\left|1 + \frac{t}{t_D}\right| \right\} \quad (3)$$

The measurements are performed discretely, so the kinetics is divided to time channels. The width of *i-th* channel is chosen varying and reciprocal to irradiation intensity (Fig. 1a). Thus, the following product is constant

$$\Delta t_i \times T_i = const \quad (4)$$

The Eq. 4 means that an irradiation exposition is constant, which determines the fluorescence signal and bleaching extent, in each channel. The applying the irradiation with pulses of equal size and width, as demonstrated in Fig. 1b, yields the same result in observed kinetics. It is a principle of pulse-position modulation approach.

The pulse positions, t_i, and channel width with conditions Eqs. 2 and 4 [1] are

$$\begin{aligned} t_i &= \alpha^i \left(t_B + \tfrac{\Delta t_0}{2}\right) - t_B \\ \Delta t_i &= \Delta t_0 \cdot \alpha^i \\ \alpha &= 1 + \tfrac{\Delta t_0}{t_B} \end{aligned} \quad (5)$$

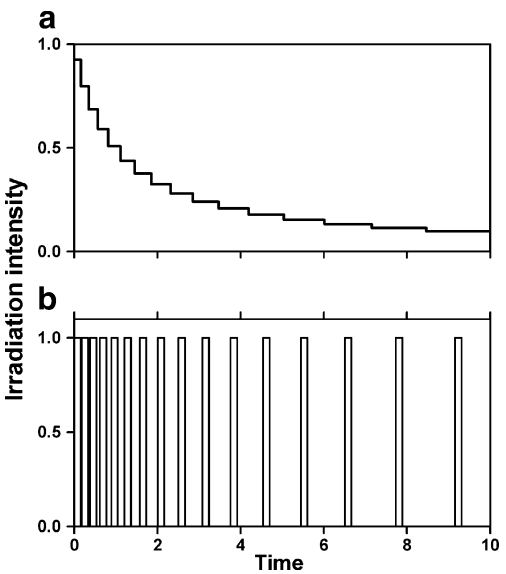

Fig. 1 The comparison of amplitude (AM) and pulse-position modulation (PPM) approaches. **a** The amplitude modulation as hyperbolic decay, Eq. 2. The sampling time/channel width increases reciprocally to intensity, Eq. 4. The central positions of channels are determined by Eq. 5. **b** The pulse-position modulation approach. The pulses are equal and centered as for AM approach

The irradiation function can be expressed as:

$$T(t) = \tau \cdot \sum_{i=0}^{N-1} \delta(t - t_i) \tag{6}$$

where τ is pulse width, it could be equal or less to the initial channel width, Δt_0; N is pulse number.

The evaluation of Eq. 1 with the result of Eq. 6 yields

$$f(t_i) = f_0 \left(1 - B \cdot \tau \cdot \left[\sum_{j=0}^{i-1} \frac{1}{1 + (t_i - t_j)/t_D} + \frac{1}{2} \right] \right) \tag{7}$$

Note that the function in Eq. 7 does not explicitly contain the value of t_B, but implicitly via the pulse positions, Eq. 5. To characterize the pulse series, we will use also the value t_B as a time scale parameter. The total time of single series are usually varied from 5 to 15 of t_B values.

The linearity of irradiation is determined by stability of pulses and accuracy of timer that can be technically provided. The constant irradiation intensity results in permanent operation condition for PMT, ensuring a good linearity. The presence of background signal gives only small constant additive term. Note that in previous methods the background term increased proportionally to increase of sampling time and reached at the end of kinetics up to 20–30% of total kinetics signal [1].

The presented approach gives the possibility to make any pulse series, and we propose to use a convolution of subseries with different time parameters. Figure 2 demonstrates the example of convolution of two series. The fast kinetics (Fig. 2a) convolves with slower (Fig. 2b) yielding the series shown in Fig. 2c. The initial channel width for slow kinetics is equal to the duration of faster kinetics. It allows excluding overlapping of fast series.

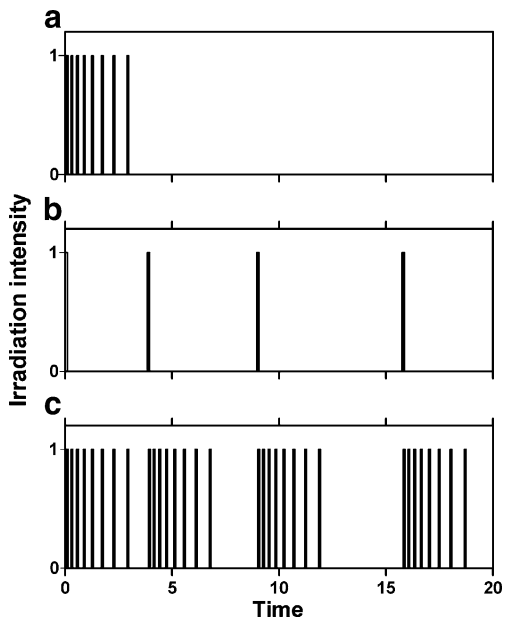

Fig. 2 The principle of series convolution. **a** Fast series: $T^a(t) = \tau \cdot \sum_i \delta(t - t_i^a)$· **b** Slow series: $T^b(t) = \tau \cdot \sum_j \delta\left(t - t_j^b\right)$. **c** The resulted convolution of two series. $T(t) = \tau \cdot \sum_i \sum_j \delta\left(t - t_i^a - t_j^b\right)$

The underlying idea of such convolution is to separate experimentally fast and slow fractions of kinetics. The low kinetics can be register as long as necessary with accumulation of fast kinetics.

Results

Measurement of diffusion of FITC labeled albumin in the glycerol/water mixture

As a simple model system we measured the diffusion FITC labeled albumin in the glycerol/water mixture (80% w/w). The value of diffusion coefficient of 5.6×10^{-9} cm^2/s (at 25 °C) was taken from our previous work [2] where it was measured by light scattering method. This value was used as reference for present photobleaching measurements.

The applied pulse series was a convolution of two series similar to shown in Fig. 2. The time parameters were for fast series: t_B=10 s, N=64, for slow series: t_B=500 s, N=8. Pulse width τ of 300 ms. Pinhole size of 0.9 mm.

The experimental kinetics is shown in Fig. 3a. In fact, this kinetics can be fitted with Eq. 7 if the only single component diffusion takes place. In presented experiment, at least one more process revealed in longer time scale. The applying of series convolution allows to separate these kinetics by corresponding averaging over each subseries. Figure 3b demonstrates the kinetics, which is averaged sum of fast subkinetics. This kinetics reflects the diffusion process and was fitted with following equation:

$$\frac{f(t_i)}{f_0} = 1 - B \cdot \tau \left(\cdot \left[\sum_{j=0}^{i-1} \frac{1}{1 + (t_i - t_j)/t_D} + \frac{1}{2} \right] + \alpha \cdot \left(i + \frac{1}{2} \right) \right) \tag{8}$$

The last term in the equation accumulates all the averaging in the longer time scale and does not interfere with the main function for diffusion. The value of this cumulative parameter is not so important; the important is that one can obtain the valid value of t_D neglecting consideration a slower effect. The data fitting yields the value t_D=11±1 s and B=0.015± 0.002 s^{-1}. The measurement with pinhole of 0.45 mm yields the value t_D=2.6±0.5 s and B= 0.015+0.003 s^{-1} that support the diffusive nature of this kinetics.

Figure 3c demonstrates the slow fraction of kinetics calculated as averaging of data within fast subkinetics. In this case, the diffusion process is neglected. This slow kinetics is a result of photobleaching of FITC labeled albumin absorbed on

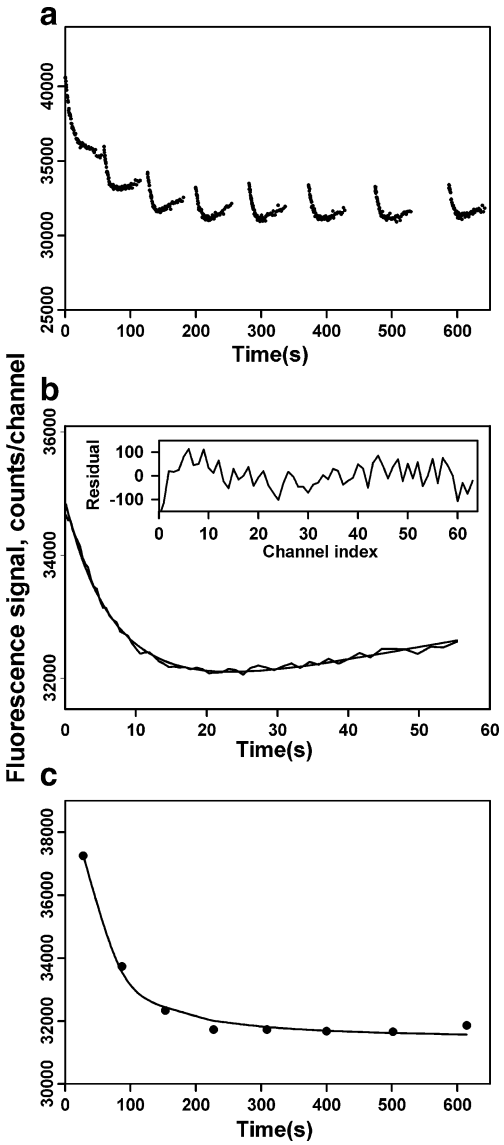

Fig. 3 The fluorescence photobleaching measurement of FITC-HSA in the water/glycerol mixture (80% w/w). **a** Total experimental fluorescence kinetics under applying of pulse series convolution. **b** The fast fraction of kinetics calculated as averaged sum of fast subkinetics. Data were fitted with Eq. 8 and yields the value t_D=11± 1 s and B=0.015±0.002 s^{-1}. **c** The slow fraction of experimental kinetics calculated as averaging of each fast subkinetics. Data were fitted with Eq. 9 and yields the immobile fraction of ~10%

the glass surface. The data fitting of immobile fraction requires, in general, applying the accurate solution [1]:

$$\left.\frac{f(t_j)}{f_0}\right|_{immobile} = \frac{1-\exp\{-2B\cdot N\cdot\tau(j+1/2)\}}{2B\cdot N\cdot\tau(j+1/2)} \tag{9}$$

where j is index in slow series; N is pulse number in fast series.

The kinetics of diffusion is performed in the approximation of low bleaching. As the dimensionless parameter of smallness, the value of $B\times t_D$ can be taken, which is, obviously, does not suite for bleaching of immobile fraction. In this case, the parameter of smallness is the value $B\times N\times M\times\tau$ ($N\times M$ – total pulse number) as one can be deduced from Eq. 9.

There is a conceptual difference from FRAP method where the immobile fraction is determined from the difference of asymptotic and prebleach intensities which both are constant values. In presented method, there is no necessity for predkinetics measurements but it is necessary to determine the asymptotic behavior of kinetics.

The analysis of slow kinetics yields the value of ~10% for immobile fraction. However, the deeper analysis of all corresponding experimental data allowed us to propose the presence of kinetics in longer time scale. It could be the kinetics of adsorption/desorption of albumin on glass surface or direct flow of solution.

Measurements of diffusion FITC-DMPE in the lipid multibilayer

For the diffusion measurements of FITC-DMPE in the multibilayer liposomes form POPC, we applied the same pulse series and spot size as for previous experiment. The experimental and reduced kinetics are shown in Fig. 4.

The fitting of fast kinetics (Fig. 4b) yields a t_D value of 1.2±0.2 s. Using previous calibration, this value corresponds to diffusion coefficient of $(6\pm1)\cdot10^{-8}$cm^2/s, which is in a good agreement with literature data [3]. The calculated value of bleaching rate of 0.03±0.002 s^{-1} is twice higher then that in the water/glycerol mixture. It could be result of albumin protection of fluorophore (due to SH groups or sterically) against photobleaching.

The slow kinetics (Fig. 4c) also demonstrated the slight decay similar to above data. In this system, the immobile is not presented. It was proposed that it is a result of loss of total fluorophore contents that should occur in limited area. It was supported by experiments on liposomes of different sizes. Approximately, the loss of total fluorophore contents that can be expressed as:

$$Q(t_j) = Q_0\frac{1-\exp\left\{-\gamma\cdot 2B\cdot N\cdot\tau(r/R)^2(j+1/2)\right\}}{\gamma\cdot 2B\cdot N\cdot\tau(r/R)^2(j+1/2)} \tag{10}$$

where $Q(t)$ is total quantity of fluorophore in the liposome; $(r/R)^2$ – is a ratio of areas of spot (size of r) to area of liposome (size of R); γ – is dimensionless correction parameter.

However, the data fitting (Fig. 4c) showed that the kinetics asymptotically does not decay to zero as predicted by Eq. 10. The additional experiments and more comprehensive data analysis allowed proposing the existence of

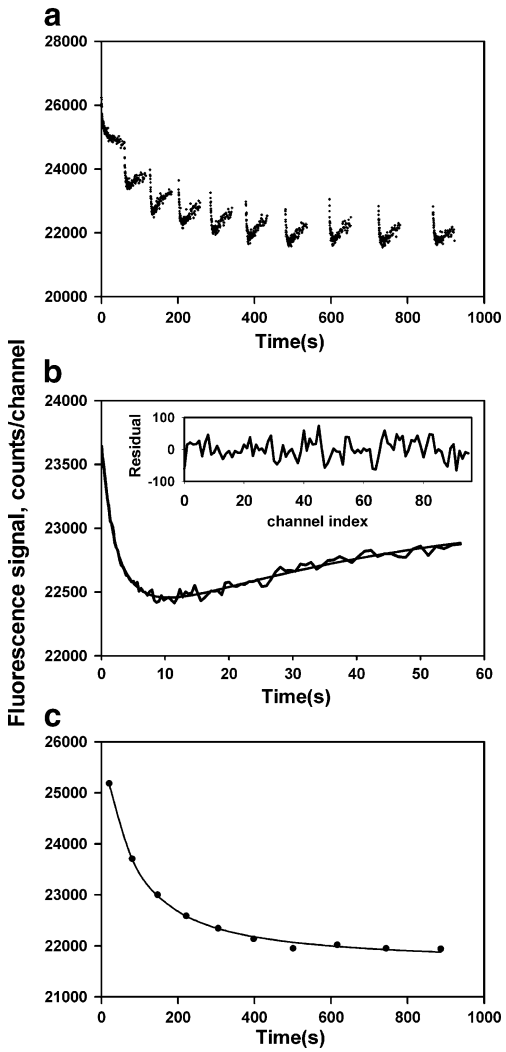

Fig. 4 The fluorescence photobleaching measurement of FITC-DMPE in the POPC liposomes. The applied series and spot size are the same as for experiment demonstrated in Fig. 3. **a** Total experimental kinetics. **b** Fast kinetics fraction. Data fitting yields the value of t_D=1.2±0.2 s, B=0.03±0.006 s^{-1}. **c** Slow kinetics fraction. Data was fitted by Eq. 10

kinetics in longer time scale. It could be a very slow diffusion process or slight movement of liposomes.

Detection the reversible fluorescence kinetics

The application of series with shorter pulse revealed the fluorescence kinetics in millisecond time scale. This phenomenon is known as reversible photobleaching and is proposed as triplet relaxation process [4]. This effect is also observed in FRAP method and usually considered as undesirable because it could interfere with diffusive kinetics under some conditions [5–7]. Using classical methods one can usually measure either kinetics of diffusion or reversible fluorescence kinetics. In the present approach, such measurements could be performed simultaneously and analyzed without interference.

Discussion

The underlying motivation of this work was to overcome the technical limitations of FRDP method, originated mainly from non-linearity, by means of methodical modification. It was successfully done by application of pulse-position modulation approach that is widely used in the different branches of techniques and science.

The providing series of equal pulses with varying distance is easier and more accurate then the amplitude modulation. Even the comparatively simple FRAP method requires two predefined intensities, bleaching and probing. Here all we need is to switch on and of the light source using programmable timer. It is especially very convenient using ultra bright LED. The application of LEDs seems very promising for fluorescence microscopy studies, however, for photobleaching experiments the intensity of irradiation is desired to be higher. The rate of photobleaching is characterized by value B, which in present experiments is 0.02–0.03 s^{-1}. In our previous work with argon laser [1], this value was 2–3 s^{-1} that allowed measuring fast diffusive kinetics (t_D=80 ms) with bleaching depth about 30%. The parameter of smallness, as mentioned above, is a product $B \times t_D$, which correlates with bleaching depth in observed kinetics. It means that to have a significant bleaching depth for data analysis, we can reasonably measure only slow diffusion with value of t_D from few seconds and more. It suits for protein diffusion measurements in the native biological membrane where $D=10^{-9}-10^{-11}$ cm^2 s^{-1}. But definitely this approach can be easily applied on argon laser based setup with acousto-optic modulator that is commonly used for FRAP techniques. More promising seems the application of diode laser with power of few milliwatts because this approach does not require intense short pulse.

The pulse approach is preferable for investigation of living cells because it causes less damage then continuous irradiation [8]. The intensity of pulses is, at least, in ten times less the bleaching pulse in FRAP method, which is usually considered as main damaging factor. The constant intensity of pulse provides the constant geometry of bleached spot during all data acquisition. In FRAP method, the spot geometry produced by intense pulse could differ from that of probing irradiation.

The methods with permanent bleaching/probing irradiation require knowing the dominant stoichiometry of photobleaching reaction. It was specially mentioned in our previous work with decaying bleaching irradiation [1] and in the approaches, applying continuous photobleaching (CP) [9, 10]. As a rule, this reaction is of first order on

irradiation intensity and fluorophore concentration, assuming dominant oxygen dependent mechanism [11] and single-photon absorption. However, the deviations take place in some cases such as oxygen free conditions [12] and two-photon photobleaching approach [13, 14]. In pulse method, the observed kinetics is actually the same as for first-order photobleaching reaction. The difference results only in the profile of bleached spot during short pulse. It requires the correction in calculation of absolute value of diffusion, if one wants to do it using profile parameters. But it is more reasonable to use the reference sample, as was performed in present work. Note, that in present experiments the spot profile is not Gaussian but rather uniform broadened by diffraction. Anyway, the hyperbolic function as kernel, Eqs. 7 and 8, yields the perfect fitting of experimental data (inserts in Figs. 3 and 4).

In the common case, the Eq. 7 can be written as:

$$f(t_i) = f_0\left(1 - B\cdot\tau\cdot\left[\sum_{j=0}^{i-1} K\left(t_i - t_j\right) + \frac{1}{2}\right]\right) \qquad (11)$$

Kernel function *K(t)* in Eq. 11 is a kinetics for single delta function of *T(t)*. In general, it could be any solution for diffusion (classical, anomalous, pattern photobleaching), chemical reaction [15], enzyme activity [16] or time-resolved polarization decay [17]. Time positions of pulses can be taken in correlation to the kernel function.

The resulted pulse series is a convolution of subseries, which one can be independently tuned, according to investigated process. The only requirement is a different time scales of these kinetics. Thus, such convolution can be considered as a scanning tool of biological system to detect and investigate the fluorescence kinetics in the wide range of time scales. For example, having enough power of LED, we could measure the reversible photobleaching, fluorophore diffusion and kinetics in longer time scale by applying of convolution of three corresponding subseries.

References

1. Glazachev YI, Khramtsov VV (2006) Fluorescence recovery under decaying photobleaching irradiation: concept and experiment. J Fluoresc 16:773–781
2. Glazacheff YI, Weiner LM, Gulyaeva LF, Lyakhovich VV (1991) Lateral mobility of cytochrome-b_5 in the lipid multibilayers. Biologicheskie membrany (Biol membr, Russian) 8:407–411
3. Kahya N, Schwille P (2006) How phospholipid-cholesterol interactions modulate lipid lateral diffusion, as revealed by fluorescence correlation spectroscopy. J Fluoresc 16:671–678
4. Periasamy N, Bicknese S, Verkman AS (1996) Reversible photobleaching of fluorescein conjugates in air-saturated viscous solutions: singlet and triplet state quenching by tryptophan. Photochem and Photobiol 63:265–271
5. Koppel DE, Axelrod D, Schlessinger J, Elson EL, Webb WW (1976) Dynamics of fluorescence marker concentration as a probe of mobility. Biophys J 16:1315–1329
6. Periasamy N, Verkman AS (1998) Analysis of fluorophore diffusion by continuous distributions of diffusion coefficients: application to photobleaching measurements of multicomponent and anomalous diffusion. Biophys J 75:557–567
7. Andrea LS, Axelrod D (1995) Spontaneous recovery of fluorescence by photobleached surface-adsorbed proteins. Photochem and Photobiol 62:239–244
8. Peters R (1981) Translational diffusion in the plasma-membrane of single cells as studied by fluorescence microphotolysis. Cell Biol Int Rep 5:733–760
9. Endress E, Weigelt S, Reents G, Bayerl TM (2005) Derivation of a closed form analytical expression for fluorescence recovery after photo bleaching in the case of continuous bleaching during read out. Eur Phys J E Soft Matter 16:81–87
10. Wachsmuth M, Weidemann T, Muller G, Hoffmann-Rohrer UW, Knoch TA, Waldeck W, Langowski J (2003) Analyzing intracellular binding and diffusion with continuous fluorescence photobleaching. Biophys J 82:1828–1834
11. Song L, Varma CA, Verhoeven JW, Tanke HJ (1996) Influence of the triplet excited state on the photobleaching kinetics of fluorescein in microscopy. Biophys J 70:2959–2968
12. Corbett JD, Cho MR, Golan DE (1994) Deoxygenation affects fluorescence photobleaching recovery measurements of red cell membrane protein lateral mobility. Biophys J 66:25–30
13. Brown EB, Wu ES, Zipfel W, Webb WW (1999) Measurement of molecular diffusion in solution by multiphoton fluorescence photobleaching recovery. Biophys J 77:2837–2849
14. Waharte F, Brown CM, Coscoy S, Coudrier E, Amblard F (2005) A two-photon FRAP analysis of the cytoskeleton dynamics in the microvilli of intestinal cells. Biophys J 88:1467–1478
15. Lele TP, Ingber DE (2006) A mathematical model to determine molecular kinetics rate constants under non-steady state conditions using fluorescence recovery after photobleaching (FRAP). Biophys Chem 120:32–35
16. Combs CA, Balaban RS (2001) Direct imaging of dehydrogenase activity within living cells using enzyme-dependent fluorescence recovery after photobleaching (ED-FRAP). Biophys J 80:2018–28
17. Buehler Ch, Dong CY, So PTC, French T, Gratton E (2000) Time-resolved polarization imaging by pump-probe (stimulated emission) fluorescence microscopy. Biophys J 79:536–549